Experimental Investigation of Geochemical Rock-Fluid Interactions During CO_2 Storage with SO_2 Impurities

Introduction

Geological CO_2 storage involves a sophisticated hierarchy of trapping mechanisms, including structural, residual, solubility, and mineral trapping. For a large-scale economic deployment of CO_2 storage, the injected CO_2 streams typically contain various reactive impurities. Consequently, the presence of impurities, such as SOx, must be carefully accounted for, as their reactive nature can significantly influence the geochemical stability of the storage reservoir (Talman, 2015).

Research utilizing full activity correction calculations has shown that incorporating just 1% SO_2 into a CO_2 stream can trigger a sharp pH drop of 2.5 units in the aqueous phase relative to pure CO_2 systems (Ellis et al., 2010). This intense acidification is driven by the superior solubility and reactivity of SO_2. Experimental data demonstrate that at room condition, SO_2 solubility exceeds that of CO_2 by approximately 30-40 times, with the solubility ratio between them increases with temperature, but decreases with pressure (Zhou et al., 2020). The high aqueous solubility and reactivity of SO_2 also promotes the transformation of sulfur species into insoluble minerals, like gypsum, fundamentally modifying the reservoir's pore structure (Glezakou et al., 2012).

Despite the critical nature of impurity-driven geochemical responses, most existing batch studies have primarily utilized low-salinity brines and relatively high impurity concentrations to simulate underground rock-fluid interactions. Such conditions may not adequately reflect the complex geochemical processes occurring in specific high-salinity storage sites. Consequently, this study addresses this knowledge gap by targeting some typical Danish storage conditions, specifically employing a high saline environment (20 wt% NaCl) to investigate the geochemical interactions triggered by the injection of a CO_2 stream containing 1000 ppm SO_2 impurity. By shifting the focus to high-salinity, this research provides a more realistic assessment of how trace reactive compounds influence rock-fluid geochemical process in deep saline aquifers.

Method

The rock samples utilized in this study were retrieved from the Helgoland outcrop, a red sandstone formation formed during the Early Triassic period. The emergence of these strata on Helgoland Island was fundamentally driven by salt tectonics, resulting in a formation characterized by high porosity and permeability that represents a high-potential candidate for geological sequestration. Due to these favorable storage attributes, the Triassic Bunter Sandstone has been designated as the primary target for the Endurance saline aquifer CO_2 storage project in the UK Southern North Sea; consequently, the Helgoland outcrop is frequently employed by researchers as a representative analog to investigate the structural integrity and reservoir heterogeneity of the target formation. For the current experimental work, the rock was processed into 1.5 cm^3 cubes, with their mineralogical compositions characterized via X-ray diffraction (XRD) and scanning electron microscope (SEM).

The experimental apparatus was centered around a high-pressure reaction cell integrated with an injection cylinder, temperature-regulated heat bath, and real-time monitoring systems for pressure and temperature. To replicate deep reservoir conditions, batch experiments were conducted at 150 bar and 50°C, with temperatures maintained by a circulating fluid jacket and gas delivery handled by a Teledyne ISCO pump. A Teflon liner was placed within the cell to isolate the 150 ml of 20 wt% NaCl brine from the reactor walls, preventing corrosion under the highly acidic conditions induced by SO_2 impurity. Each test involved two rock cubes, beginning with a three-day N_2 soak to establish a mineral dissolution baseline under non-reactive conditions. Following a vacuum phase to remove N_2, the cell was charged with the impure CO_2 mixture for a 21-day reaction period. Brine aliquots (2–3 ml) were sampled bi-weekly and analyzed for pH and ion concentrations via pH meter and ICP-OES. Upon completion, the rock cubes underwent a rigorous cleaning protocol—soaking in deionized water for 48 hours with 12-hour water exchanges to eliminate halite precipitation that might otherwise obscure post-reaction SEM and micro-CT characterizations. Bulk mineralogical transformations and elemental shifts before and

after experiment will be quantified using XRD and XRF. These findings will be integrated with high-resolution SEM-EDS surface imaging and three-dimensional Micro-CT analysis to evaluate modifications in rock morphology and internal pore architecture.

Results and Discussion

Morphological observations of the rock samples via SEM imaging revealed that calcite on the rock surface, predominantly functioning as a pore-filling cement, underwent near-complete dissolution, significantly increasing the exposure of the underlying pore structure. Furthermore, polyhedral calcite crystals, originally formed through secondary over-saturation and growth, exhibited distinct reactive etching marks, confirming aggressive corrosive activity at the mineral-fluid interface (Fig. 1a, b, e). In contrast, despite their abundance in the matrix, feldspars showed no discernible alteration (Fig. 1c, d, f), a lack of reactivity that was also mirrored by the hematite phases. These solid-phase observations were complemented by aqueous monitoring, which showed that the brine pH remained remarkably stable at approximately 5.85 throughout the three-week reaction period in Figure 2. This stability is attributed to a combination of thermodynamic and mineralogical factors. Primarily, the high saline environment (20 wt% NaCl) induced a pronounced "salting-out" effect, which restricted CO_2 solubility. Consequently, the reduced proton generation from limited CO_2 dissolution, coupled with the substantial buffering capacity provided by the high calcite content within the rock matrix, effectively mitigated significant pH fluctuations during the sequestration process.

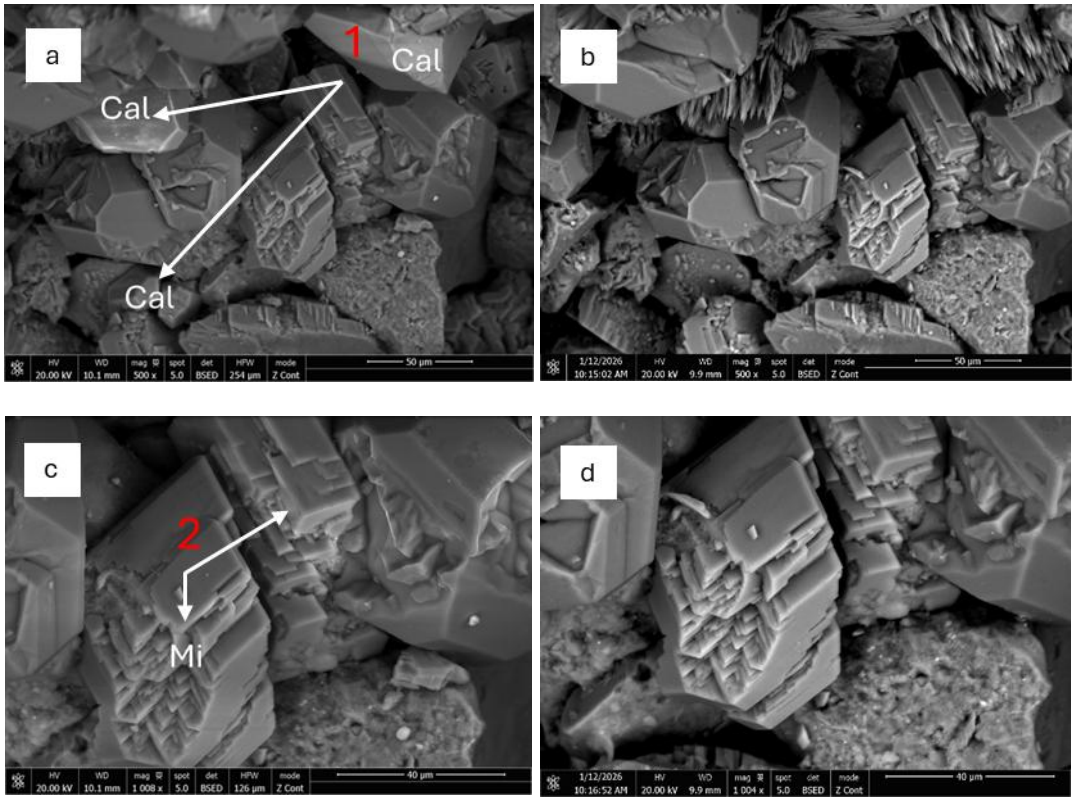

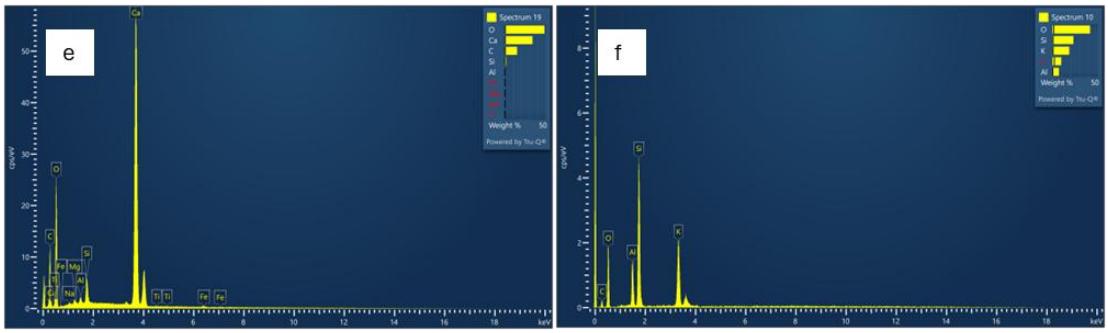

Figure 1 *BSED images and EDS characterizations for pure CO_2 experiment. (a) and (c) pre-observations of rock surface. (b) and (d) post -observations after batch experiment. (e) EDS spectra for spot 1. (f) EDS spectra for spot 2. Cal=calcite, Mi=microcline*

Brine analysis in Figure 2 via ICP-OES confirmed that mineral dissolution remained negligible during the initial N_2 soaking phase, evidenced by the presence of only trace Ca^{2+} concentrations. Transitioning to the pure CO_2 stage, however, triggered an immediate and substantial surge in Ca^{2+} levels, signaling rapid and pronounced calcite dissolution. Simultaneously, a stable but elevated Mg^{2+} concentration was observed, which, when integrated with XRD and SEM findings, can be attributed to the moderate dissolution of chamosite. Conversely, K^+ concentrations remained largely unaffected across both the N_2 and CO_2 stages, aligning with SEM observations that showed no significant feldspar (albite and microcline) degradation. Under these high-salinity conditions, the relative stability of the feldspar group is likely a result of the moderate pH environment and insufficient reaction time to overcome their slower dissolution kinetics. The geochemical profiles in Figure 3 demonstrate that SO_2 triggers far more aggressive mineral dissolution than pure CO_2. This reactivity is evidenced by a pH drop to 4.49 and a sixfold increase in Ca^{2+} concentration, signifying massive calcite dissolution. While the high abundance of calcite and feldspar provided initial pH buffering, the subsequent decline in aqueous calcium after two weeks suggests the onset of secondary gypsum precipitation. Notably, while iron was undetectable in the pure CO_2 case, SO_2 impurities promoted significant hematite dissolution, causing iron concentration to eventually surpass those of Mg and K. This anomalous enrichment is likely driven by the aggressive interaction between SO_2 impurities and hematite, a reaction pathway that remains inactive in the absence of the sulfur component.

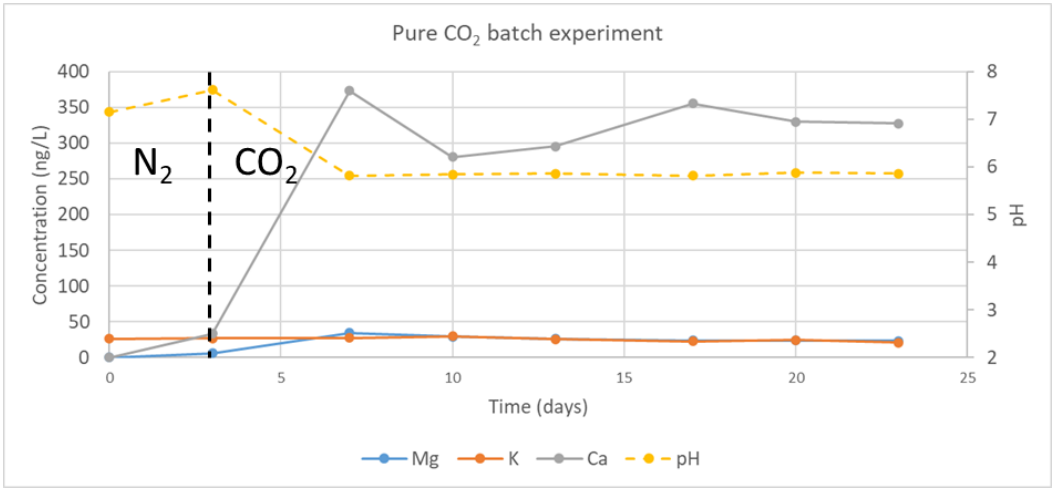

Figure 2 *Dissolved ions from brine samples for pure CO_2 batch experiment*

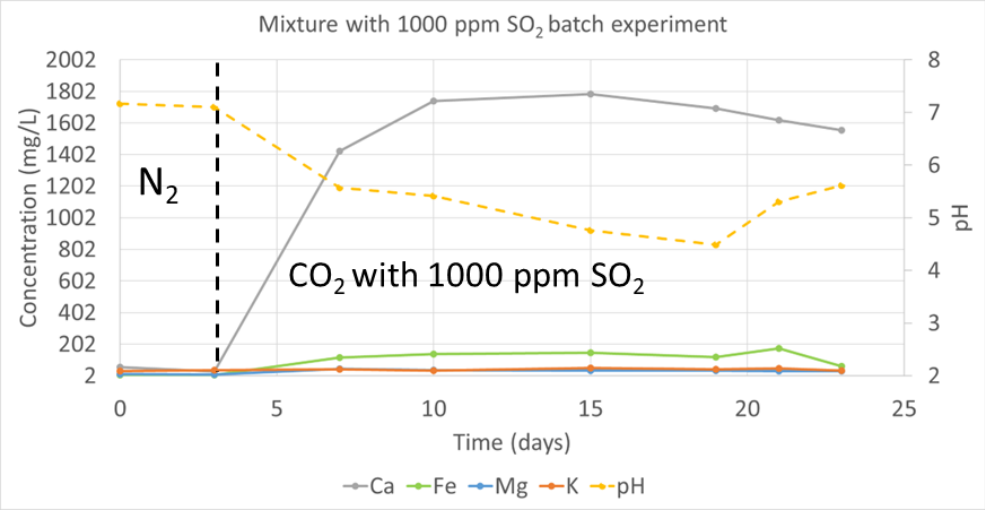

Figure 3 *Dissolved ions from brine samples for mixture batch experiment*

Conclusions

The main findings of this study can be summarized as follows:

- Dissolution was dominated by calcite, while feldspars and hematite remained stable in pure CO_2 batch experiment. The mineral buffering ensured a steady brine pH of approximately 5.85.
- The addition of 1000 ppm SO_2 caused a pH drop to ~4.49 before a slow recovery. And this impurity triggered a redox reaction in hematite.
- Although calcite and feldspar provided initial pH buffering, the eventual decline in aqueous calcium suggests a transition toward secondary gypsum precipitation.

Acknowledgements

The authors would like to acknowledge funding provided via the European Commission's Horizon Europe research and innovation program under the Marie Skłodowska-Curie Grant Agreement ID: 101118369, Material Science Innovation for Accelerated, Sustainable and Safe Implementation of Carbon Capture and Storage (MISSION-CCS).

References

Ellis, B.R., Crandell, L.E. and Peters, C.A. [2010]. Limitations for brine acidification due to SO2 co-injection in geologic carbon sequestration. *International Journal of Greenhouse Gas Control*, **4**, 575–582.

Glezakou, V.A., Peter McGrail, B. and Todd Schaef, H. [2012]. Molecular interactions of SO2 with carbonate minerals under co-sequestration conditions: A combined experimental and theoretical study. *Geochimica et Cosmochimica Acta*, **92**, 265–274.

Pearce, J.K., Kirste, D.M., Dawson, G.K.W., Farquhar, S.M., Biddle, D., Golding, S.D. and Rudolph, V. [2015]. SO2 impurity impacts on experimental and simulated CO2–water–reservoir rock reactions at carbon storage conditions. *Chemical Geology*, **399**, 65–86.

Talman, S. [2015]. Subsurface geochemical fate and effects of impurities contained in a CO2 stream injected into a deep saline aquifer: What is known. *International Journal of Greenhouse Gas Control*, **40**, 267–291.

Zhou, Q., Guo, H., Yang, P. and Wang, Z. [2020]. Solubility of SO2 in Water from 263.15 to 393.15 K and from 10 to 300 bar: Quantitative Raman Spectroscopic Measurements and PC-SAFT Prediction. *Industrial & Engineering Chemistry Research*, **59**, 12855–12861.